

Evaluation of typhoon induced fatigue damage using health monitoring data for the Tsing Ma Bridge

Tommy H. T. Chan†

*Department of Civil and Structural Engineering, The Hong Kong Polytechnic University,
Hung Hom, Kowloon, Hong Kong*

Z. X. Li‡

College of Civil Engineering, Southeast University, Nanjing, 210096, China

J. M. Ko‡†

*Department of Civil and Structural Engineering, The Hong Kong Polytechnic University,
Hung Hom, Kowloon, Hong Kong*

(Received July 24, 2003, Accepted January 8, 2004)

Abstract. This paper aims to evaluate the effect of typhoons on fatigue damage accumulation in steel decks of long-span suspension bridges. The strain-time histories at critical locations of deck sections of long-span bridges during different typhoons passing the bridge area are investigated by using on-line strain data acquired from the structural health monitoring system installed on the bridge. The fatigue damage models based on Miner's Law and Continuum Damage Mechanics (CDM) are applied to calculate the increment of fatigue damage due to the action of a typhoon. Accumulated fatigue damage during the typhoon is also calculated and compared between Miner's Law and the CDM method. It is found that for the Tsing Ma Bridge case, the stress spectrum generated by a typhoon is significantly different than that generated by normal traffic and its histogram shapes can be described approximately as a Rayleigh distribution. The influence of typhoon loading on accumulative fatigue damage is more significant than that due to normal traffic loading. The increment of fatigue damage generated by hourly stress spectrum for the maximum typhoon loading may be much greater than those for normal traffic loading. It is, therefore, concluded that it is necessary to evaluate typhoon induced fatigue damage for the purpose of accurately evaluating accumulative fatigue damage for long-span bridges located within typhoon prone regions.

Key words: typhoon; long-span bridge; fatigue damage; stress spectrum; health monitoring.

† Associate Professor

‡ Professor

‡† Chair Professor and Dean

1. Introduction

Several studies have been undertaken on the estimation of wind-induced fatigue damage in cable-stayed bridges, e.g. Virlogeux (1992) and Gu *et al.* (1999). These works firstly evaluated wind load with different speed and direction, and then calculated the buffeting response of the bridge. Although the wind load model has been developed by considering many factors and includes wind buffeting, it is still unable to obtain an accurate evaluation of realistic response for a bridge under the passage of a typhoon. The best method available to obtain the realistic response of a bridge under typhoon conditions is to carry out field measurements for the bridge. However, it is difficult to carry out field testing when a typhoon or severe tropical storm passes over the bridge to be tested since all actions on the bridge have to be stopped during a typhoon.

With the development of the structural health monitoring system for long-span suspension bridges (Aktan *et al.* 1998), it becomes possible to obtain field data of dynamic responses induced by a typhoon for bridges with a permanent installed monitoring system. Studies have been made on how to take full advantage of on-line monitoring data for the purpose of evaluating fatigue damage of bridge-deck sections under normal traffic loading (Chan *et al.* 2000, Li *et al.* 2000), which consists of both railway and road traffic, and is defined as the traffic loading on the bridge under normal working conditions. This paper discusses how to evaluate typhoon induced fatigue damage based on the structural health monitoring data. The strain-time histories measured by the system permanently installed on the Tsing Ma Bridge (TMB) during two typical typhoons under the hoisting of Typhoon Signal No. 9 or 10 are investigated. The increment of fatigue damage due to the typhoon is then evaluated by applying the fatigue models based on Miner's Law and Continuum Damage Mechanics (CDM) respectively.

2. Typhoons in Hong Kong

Typhoons are very common in Hong Kong during May to November each year. There have been many severe tropical cyclones and typhoons which have affected Hong Kong since May 22, 1997, when the Tsing Ma Bridge (TMB) was commissioned. According to the records held by the Hong Kong Observatory, the details of typhoons requiring the hoisting of the Hurricane Signal No. 8 or over, in Hong Kong during 1997-2002 is shown in Table 1. This Table identifies that three typhoons, Victor, Maggie and York, are typical and should be analyzed further since they are the most severe typhoons on record. Typhoon Victor crossed over the TMB on 2 August 1997 just after the structural health monitoring system for the bridge had been installed. As a result, the monitoring data, especially the structural response data, was not completely recorded. Therefore, as typical examples of typhoons in Hong Kong, the two other major typhoons listed in Table 1 i.e. Maggie and York, will be analyzed in this paper.

"Maggie" entered the South China Sea on 6 June 1999 and landed over Hong Kong in the early morning of 7 June and weakened into a severe tropical storm. As Maggie moved closer to Hong Kong, local winds strengthened from the north and the Strong Wind Signal No. 3 was hoisted at 2.15 p.m. on 6 June. As Maggie came still closer that night and with gales being expected, the No. 8 NORTHWEST Gale or Storm Signal was hoisted at 0.30 a.m. on 7 June. With Maggie's landfall over Hong Kong imminent and winds strengthening even further, the Increasing Gale or Storm Signal No. 9 was hoisted at 2.45 a.m. Maggie made landfall over the Sai Kung Peninsula in Hong

Table 1 List of typhoons requiring the hoisting of Hurricane Signal No. 8 or over in Hong Kong during 1997-2002 (after [HREF 1])

Intensity	Name	Signal	Issued		Cancelled		Duration hh mm
			hh mm	dd/mon/yyyy	hh mm	dd/mon/yyyy	
Typhoon	VICTOR	8 NE	12:00	02/Aug/1997	16:50	02/Aug/1997	04 50
Typhoon	VICTOR	9	16:50	02/Aug/1997	23:40	02/Aug/1997	06 50
Typhoon	VICTOR	8 SW	23:40	02/Aug/1997	03:30	03/Aug/1997	03 50
Typhoon	LEO	8 NE	13:30	02/May/1999	17:30	02/May/1999	04 00
Typhoon	MAGGIE	8 NW	00:30	07/Jun/1999	02:45	07/Jun/1999	02 15
Typhoon	MAGGIE	9	02:45	07/Jun/1999	05:45	07/Jun/1999	03 00
Typhoon	MAGGIE	8 NE	05:45	07/Jun/1999	10:30	07/Jun/1999	04 45
Typhoon	SAM	8 NW	12:30	22/Aug/1999	20:10	22/Aug/1999	07 40
Typhoon	SAM	8 SW	20:10	22/Aug/1999	03:50	23/Aug/1999	07 40
Typhoon	YORK	8 NW	03:15	16/Sep/1999	05:20	16/Sep/1999	02 05
Typhoon	YORK	9	05:20	16/Sep/1999	06:45	16/Sep/1999	01 25
Typhoon	YORK	10	06:45	16/Sep/1999	17:45	16/Sep/1999	11 00
Typhoon	YORK	8 SW	17:45	16/Sep/1999	22:10	16/Sep/1999	04 25
Severe Tropical Storm	CAM	8 NW	05:20	26/Sep/1999	11:20	26/Sep/1999	06 00
Severe Tropical Storm	CAM	8 SW	11:20	26/Sep/1999	14:10	26/Sep/1999	02 50
Typhoon	UTOR	8 NE	19:30	05/Jul/2001	23:40	05/Jul/2001	04 10
Typhoon	UTOR	8 NW	23:40	05/Jul/2001	09:40	06/Jul/2001	10 00
Typhoon	UTOR	8 SW	09:40	06/Jul/2001	13:40	06/Jul/2001	04 00
Typhoon	YUTU	8 NE	00:30	25/Jul/2001	10:40	25/Jul/2001	10 10
Typhoon	YUTU	8 SE	10:40	25/Jul/2001	19:40	25/Jul/2001	09 00
Severe Tropical Storm	HAGUPIT	8 SE	13:40	11/Sep/2002	01:40	12/Sep/2002	12 00

Kong some thirty minutes after the hoisting of the No. 9 signal. It traversed Hong Kong from northeast to southwest at about 30 km/h before moving to offshore waters. Maggie was closest to the Hong Kong Observatory Headquarters at around 4 a.m. when it was about 5 km to the northwest. During its passage, Maggie brought frequent squalls and heavy rain to Hong Kong. The trace of Maggie over Hong Kong is shown in Fig. 1.

“York” developed as a tropical depression about 420 km northeast of Manila on 12 September 1999, and strengthened into a severe tropical storm on 14 September. The No. 8 NORTHWEST Gale or Storm Signal was hoisted at 3.15 a.m. on 16 September. Winds strengthened rapidly in the next few hours. The Increasing Gale or Storm Signal No. 9 was hoisted at 5.20 a.m. and the Hurricane Signal No. 10 at 6.45 a.m. The signal was in force for 11 hours. Winds of hurricane force, firstly northeasterly and then southwesterly, buffeted Hong Kong on 16 September. Local winds experienced a temporary lull during the eye’s passage. The eye of York was closest to the Hong Kong Observatory Headquarters at around 10 a.m. when it was about 20 km to the south-southwest. As shown in Fig. 1, York crossed over Hong Kong from southeast to northwest. The

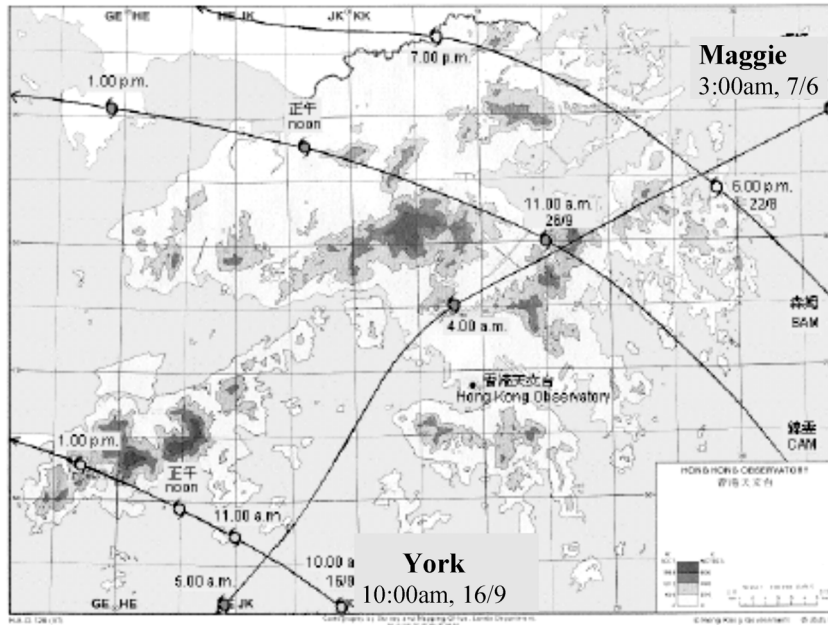


Fig. 1 Tracks of Maggie and York over Hong Kong

alignment of the deck of the TMB deviates from the east-west axis by about 17° anti-clockwise (see Fig. 2). In fact, most of Hong Kong's major typhoons including York will follow a track affecting the bridge in a way as a direct hit. From the above point of view, York is typical for investigating the effect of typhoons crossing Hong Kong on the Tsing Ma Bridge.

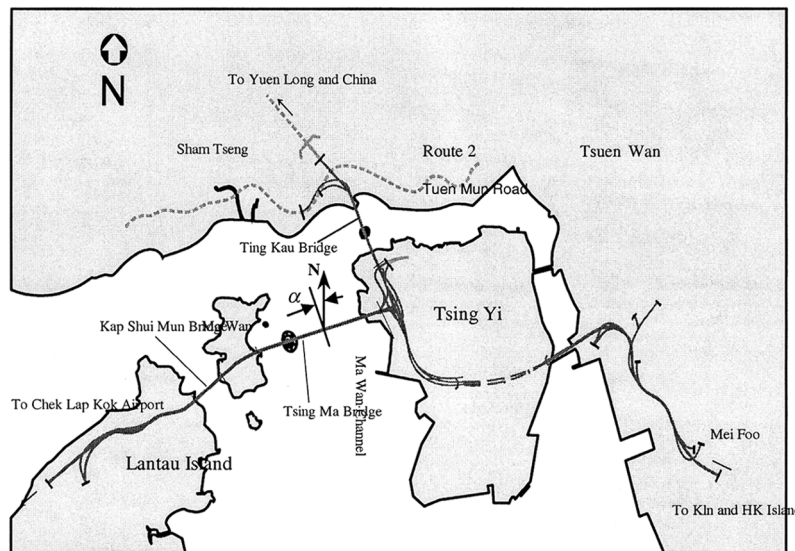


Fig. 2 Location plan of Tsing Ma Suspension Bridge

3. Wind and strain response monitoring

The Tsing Ma Bridge (TMB) is the longest suspension bridge in the world that carries both highway and railway traffic. It can be seen from Fig. 2 that the bridge serves as a main section of the Lantau Link supporting highway and railway transport between Tsing Yi Island and Lantau Island. For safety assurance, a structural monitoring system - Wind And Structural Health Monitoring System (WASHMS) has been devised by the Highways Department of the Hong Kong SAR Government (Lau *et al.* 2000) to monitor the integrity, durability and reliability of the bridge (Fig. 3). The bridge has a double deck configuration with the expressway on the upper deck and the railway below. Structurally, the deck section of the Tsing Ma Bridge is a hybrid arrangement combining both truss and box forms, Lau *et al.* (1997).

The WASHMS for the Tsing Ma Bridge includes six anemometers including two digital ultrasonic anemometers installed on the north side and south side of the bridge deck at the mid-span, specified respectively as WITJN01 and WITJS01 (Fig. 4). Each ultrasonic anemometer can measure three components of wind velocity simultaneously. Figs. 5(a) and 5(b) show variations of 10-minute-averaged mean wind speed and direction, respectively, for the data obtained from the north anemometer “WITJN01” during Maggie. Figs. 6(a) and 6(b) show variations of 10-minute-averaged mean wind speed and direction, respectively, for the data obtained from the north anemometer “WITJN01” during York. In the Figures, the x -coordinate is the local time (HKT) and the measured data starts from 00:00 HKT, 16 September 1999 and ends at 20:00 HKT of the same day. The maximum 10-minute mean wind speed measured by “WITJN01” during Maggie was 14 m/s at about 4:20 HKT, 6 June 1999. In Fig. 6(b), the direction angle α is measured from north anti-clockwise as shown in Fig. 2. It can be seen that the mean wind blew, approximately from the south, across the bridge in the time region. The maximum 10-minute mean wind speed measured by “WITJN01” during York was 28.4 m/s at about 8:40 HKT, 16 September 1999.

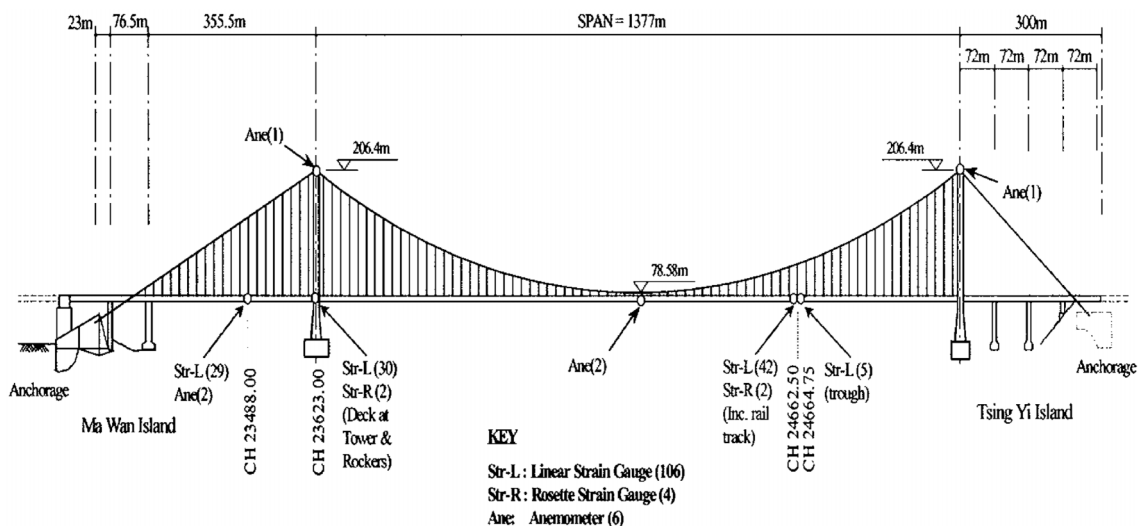


Fig. 3 Sensors layout of the Tsing Ma Bridge

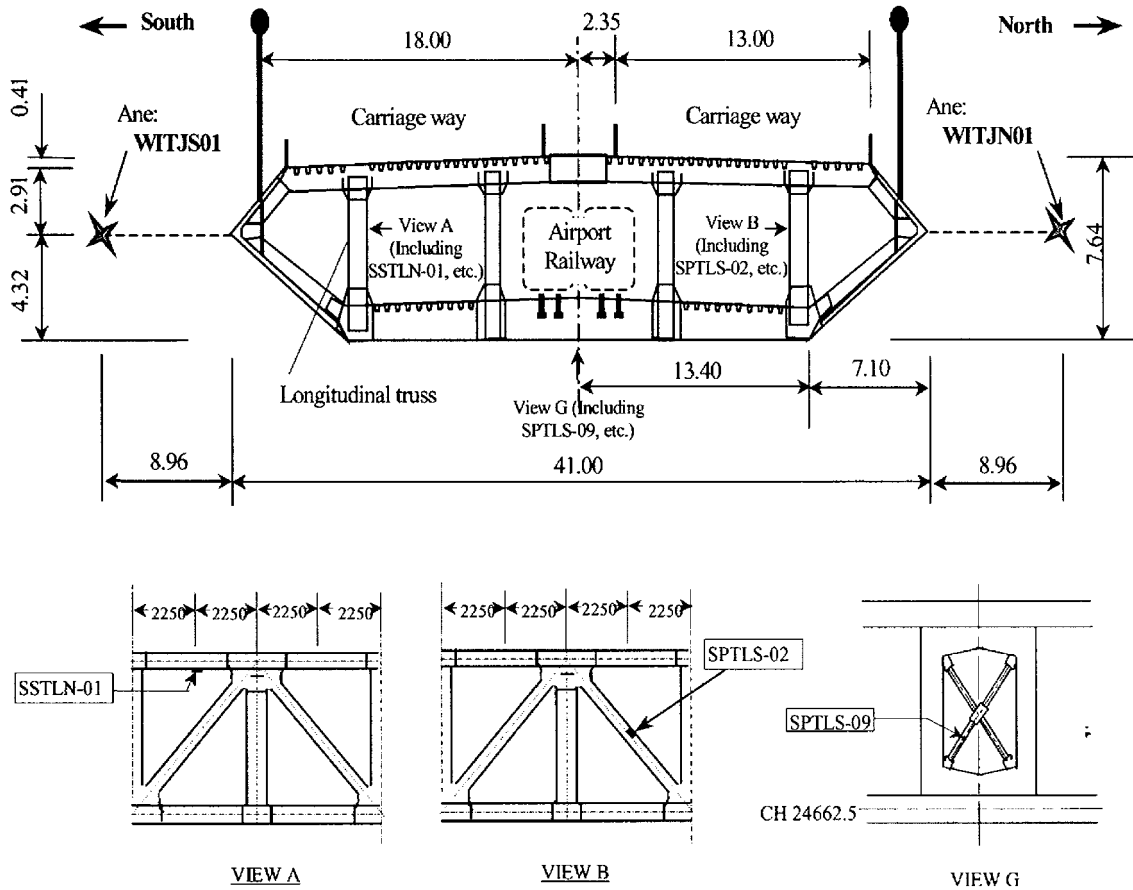


Fig. 4 Locations of strain gauges and anemometers in the cross frame

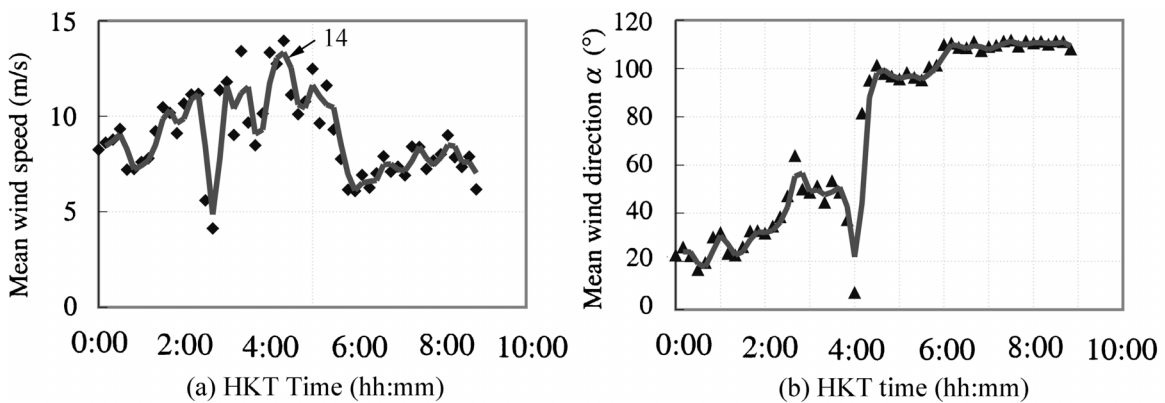


Fig. 5 Mean wind speed and direction from the anemometer “WITJN01” during Maggie: (a) 10 min mean speed, (b) 10 min mean wind direction

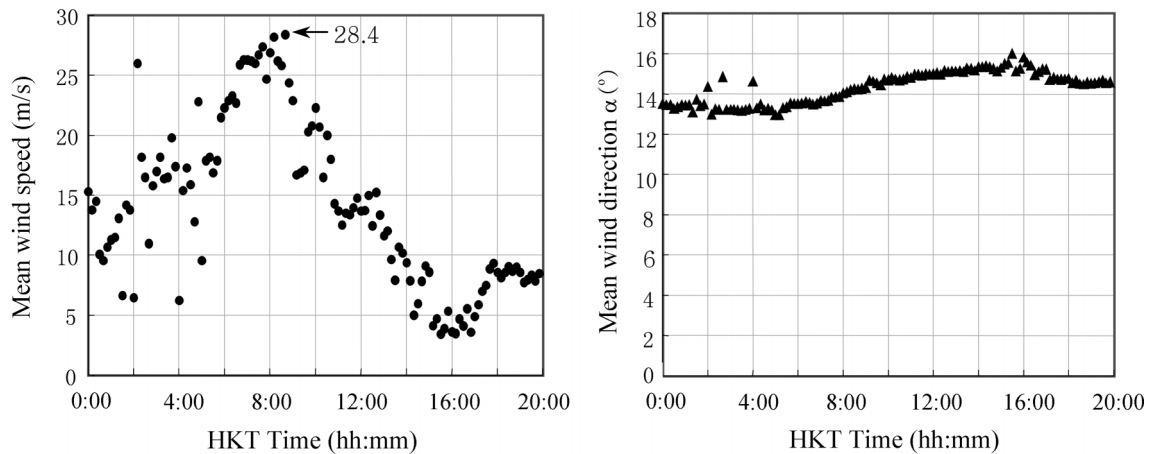


Fig. 6 Mean wind speed and direction from the anemometer “WITJN01” during York: (a) 10 min mean speed, (b) 10 min mean wind direction

4. Strain-time history during typhoons “Maggie” and “York”

Strain-time history has been recorded at strain gauge locations installed on the decks of the TMB since the bridge was commissioned. It is a useful database for on-line fatigue analysis of the bridge. The data recorded by the monitoring system for the bridge under typhoon conditions is invaluable for the analysis of typhoon induced fatigue since this data is very limited to date. In order to catch the particular features of typhoon induced strain history, strains distributed at several critical locations in a deck section are firstly studied in this section.

The most vulnerable zones may be different for different types of loading. By dealing with other data measured at different locations, the locations vulnerable both for normal traffic and under typhoon conditions are selected for comparison in the present study. According to the criticality and vulnerability ratings review by the Flint & Neill Partnership (1998), the most vulnerable zones are those under the outermost traffic lanes carrying local loads from vehicular traffic. Although the road traffic on the upper deck was stopped during periods when Typhoon Signal No. 8 or above, was raised, the locations at the two sides of the outmost deck are still critical from the point of view of aerodynamics. Railway beams made up of two inverted T-beams welded to flange plates are subjected to local loading from trains and effects of composite interaction with the main deck girders. They are prone to fatigue damage from railway loading. Based on the above review, strain histories measured by three strain gauges, set at locations A, B and G shown in Fig. 4 are selected in the study. As shown in Fig. 4, the strain gauge “SSTLN-01” is located on the top chord of the north outer longitudinal truss, “SPTLS-02” is on the left diagonal bracing of the south outer longitudinal truss and “SPTLS-09” is on the lower bracing of the cross frame underneath the railway. The analysis of fatigue damage under normal traffic loading has shown that the effective stress range at the above locations takes a comparatively large value, which means these locations are critical when the bridge serves under normal traffic and they also should be paid special attention for analysis of typhoon fatigue damage. It is observed that the strain history at “SPTLS-09” takes the most large amplitude strain range amongst the three locations. Considering that the

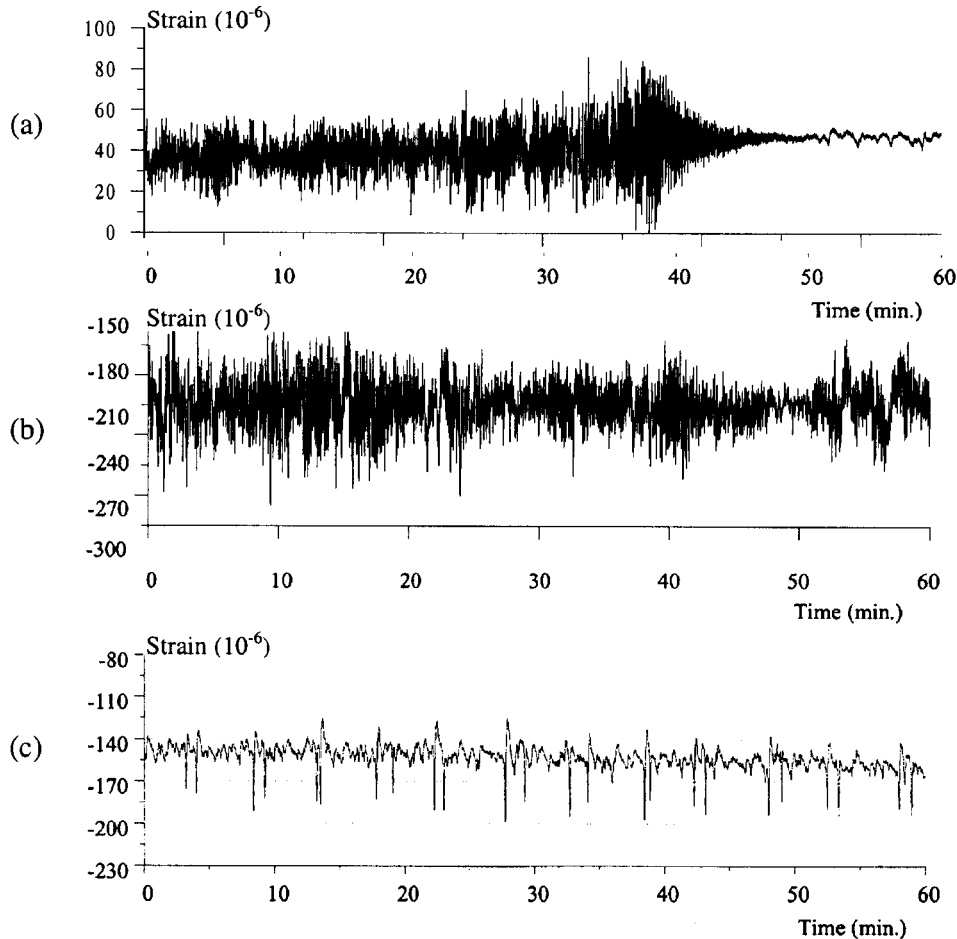


Fig. 7 Hourly strain histories at "SPTLS-09" during (a) "Maggie" (3:30~4:30), (b) "York" (8:00~9:00) and (c) Normal Traffic

train running across the bridge to Hong Kong Airport was still in service during typhoon York the above observation is understandable and the strain recorded at "SPTLS-09" has actually included the strain due to the interaction of running train and the bridge under typhoon conditions.

Fig. 7 shows hourly strain histories at "SPTLS-09" during (a) "Maggie" from 3:30 to 4:30 a.m. when the value of wind speed measured by "WITJN01" takes its maximum (as shown in Fig. 5a), (b) "York" from 8:00 to 9:00 a.m. when the value of wind speed measured by "WITJN01" takes its maximum (as shown in Fig. 6a) and (c) Normal Traffic. It is also observed that the strain history due to typhoon conditions when there was no railway service and the road was closed, has a pattern different from that due to normal traffic. The normal traffic induced strain time curve in one hour can be considered to be composed of many small pulses of strain and some higher pulses as shown in Fig. 7(c). Each higher pulse corresponds approximately to the passage of a train. The typhoon induced strain time curve has many more cycles of strain range with large amplitudes than that corresponding to passing trains. It can be found that the strain ranges during typhoon York shown in

Fig. 7(b) are higher than that during typhoon Maggie as shown in Fig. 7(a). Therefore, the analysis on fatigue damage induced by typhoons in the following section, will be carried out on the basis of the strain-time history data obtaining during the passing of typhoon York.

5. Stress ranges in hourly stress history due to the typhoon

The strain-time histories shown in Fig. 7 are composed of complicated variable-amplitude cycles. The stress-time histories can be obtained from these strain histories. In this work, the rain-flow counting method developed by Downing (1972) is used to count closed stress-strain hysteresis loops as cycles at different levels of stress range and mean stress in a block of cycles. The 3-D histograms of rain-flow counting for a block of cycles are given in Fig. 8, in which Fig. 8(a) shows stress cycles at the location of the strain gauge “SSTLN-01” for hourly stress history under “York” during

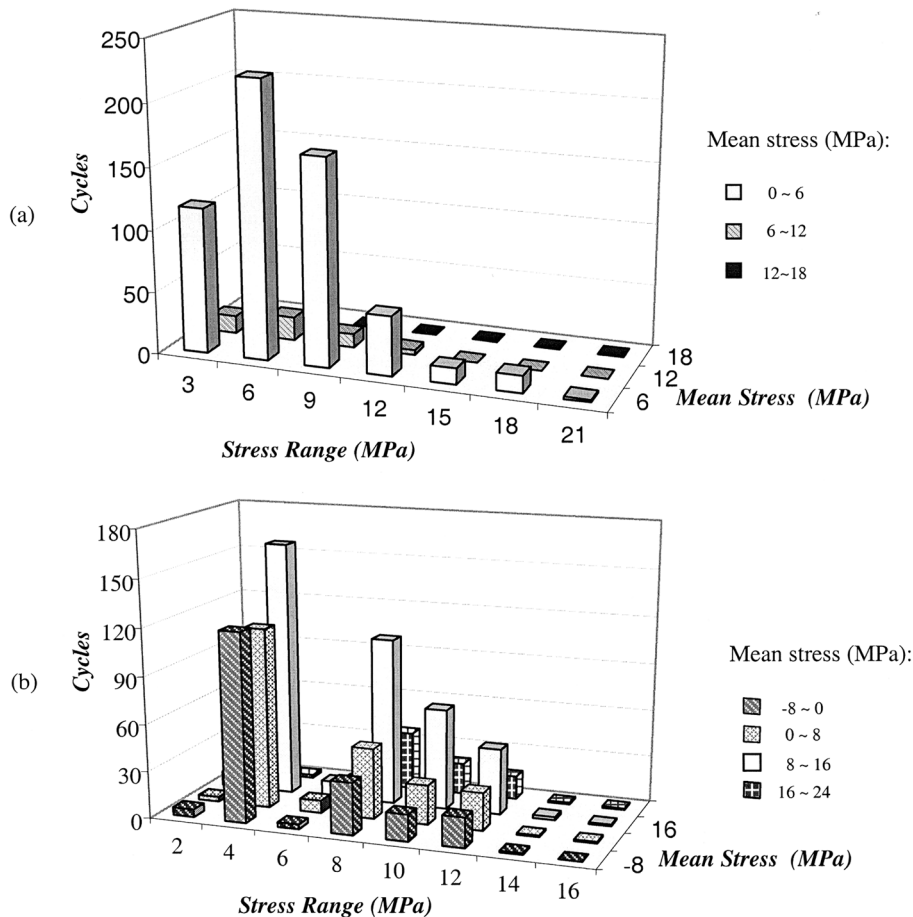


Fig. 8 Rainflow counted cycles distribution with respect to stress range and mean stress at “SSTLN-01” for (a) hourly stress history under “York” and (b) daily stress history at normal traffic

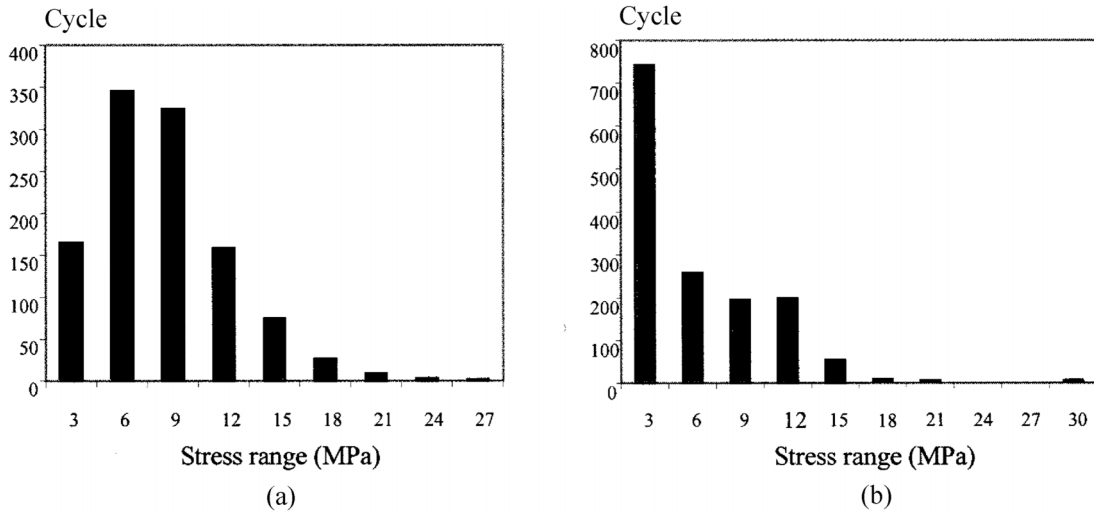


Fig. 9 Stress ranges occurred at “SPTLS-09” for (a) hourly stress history under Typhoon “York” and (b) daily stress history at normal traffic

the hour 14:00~15:00. For the purpose of comparison, the histogram of stress spectrum at the same location for daily stress history at normal traffic is also shown in Fig. 8(b). It is observed that typhoon induced stress cycles are distributed in the stress range from 3 MPa to 21 MPa, and most of the stress cycles with mean stress vary from 0~6 MPa. Only very small cycles are in the region of the mean stress over 6 MPa. This is different from the normal traffic induced stress cycles with significant variation in the value of the mean stress from -8 MPa to 24 MPa (see Fig. 8b). The above observations suggest that typhoon induced stress cycles do not have significantly fluctuating mean stress. Therefore, the effect of mean stress on fatigue damage can be neglected.

Fig. 9 shows a 2-D histogram of rain-flow counted stress spectrum at the location “SPTLS-09” for (a) hourly stress history under typhoon “York” 14:00~15:00 and (b) daily stress history under normal traffic conditions. It can be seen that the stress spectrum for typhoon induced stress cycles has more cycles in the higher stress range than that induced by normal traffic. It can also be observed that the stress spectrum for typhoon induced stress history has a pattern different from that induced by normal traffic, and both Fig. 7(a) and Fig. 9(a) show a pattern of approximate Rayleigh distribution.

The effective stress range for a variable-amplitude stress spectrum is defined as the constant-amplitude stress range that would result in the same fatigue life as the variable-amplitude spectrum (Schilling 1978). The formula for calculating the effective stress range can be written as:

$$\Delta\sigma_{ef} = \left[\frac{1}{N_T} \sum_i n_i \Delta\sigma_i^m \right]^{\frac{1}{m}} \quad (1)$$

in which, n_i is the number of cycles of stress range $\Delta\sigma_i$; $\Delta\sigma_i$ is variable amplitude stress range; N_T is the total number of cycles ($=\sum_i n_i$); and m is the slope of the corresponding constant amplitude S-N line. The effective stress range of the variable amplitude stress spectrum, $\Delta\sigma_{ef}$ from the above equation is equal to the root mean square (RMS) if m is taken as 2. If m is taken as the slope of the

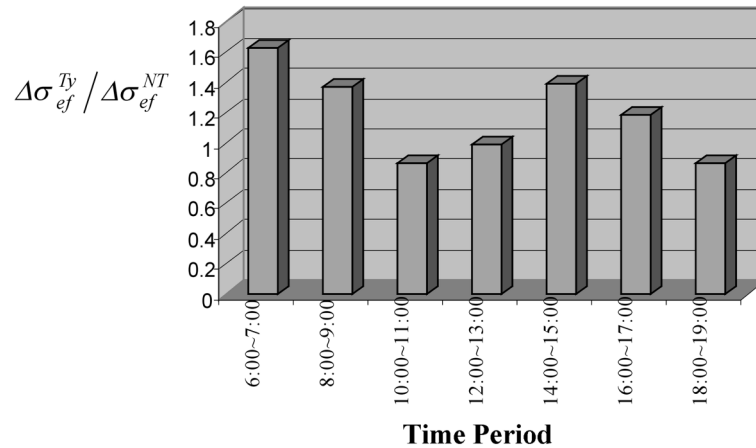


Fig. 10 Plot of normalized values of the effective stress range

constant amplitude S-N curve for the particular detail under consideration, the equation is equivalent to Miner’s Law, and for most structural details, m is about 3. The effect of the mean stress in each cycle of the variable-amplitude stress spectrum on the effective stress range is not considered in the above equation. The value of the effective stress range for a variable-amplitude spectrum can be considered as a representative value of fatigue behavior generated by the variable-amplitude spectrum at the location to be considered.

Usually, cyclic stress induced by typhoon conditions, fluctuates significantly in the amplitude of stress range and the value of the effective stress range for the hourly stress spectrum at different time periods is expected to vary significantly. In order to show the variation, some normalized values of the effective stress range for the hourly stress spectrum at different periods of time during the passage of typhoon “York” are calculated and shown in Fig. 10. In the Figure, $\Delta\sigma_{ef}^{Ty}$ expresses the value of the effective stress range for the hourly stress spectrum when typhoon “York” past the bridge on 16 Aug. 1999; while $\Delta\sigma_{ef}^{NT}$ expresses the value of effective stress range for the hourly stress spectrum under normal traffic which is almost a constant at the same time period of every day as shown in Fig. 7(c). The result of the normalized effective stress range for the hourly stress spectrum induced by the typhoon varies significantly in Fig. 10. The maximum value of the effective stress range for the stress spectrum induced by the typhoon at 6:00~7:00 is 1.629 times that for the stress spectrum under normal traffic. The effective stress range is close to that for normal traffic when a temporary lull occurred during the passage of typhoon York’s eye (10:00~13:00) and when York is over the area of the bridge. The above results of the effective stress range for hourly stress spectrum suggest that, the stress-time histories under typhoon conditions vary significantly with time. It cannot be expressed as a constant-amplitude stress range as the situation of stress-time history under normal traffic loading in which the effective stress range is obtained as a constant stress range for daily stress spectrum. It is, therefore, necessary for the typhoon loading, that the effective stress range for hourly stress spectrum is used as a constant stress range, and this constant stress range can be calculated based on the original variable-amplitude stress spectrum.

6. Evaluation of fatigue damage due to typhoon

Fatigue in bridge members is a cumulative process under high-cycle where stress fluctuation is usually low so that the deformation in the structure is elastic. Fatigue damage in the region of fatigue crack initiation and growth of cracks in micro-scale can be well described by the concept and theory of Continuum Damage Mechanics (CDM). Based on thermodynamics and potential of dissipation, the rate of damage for high-cycle fatigue has been expressed as a function of the accumulated micro-plastic strain, the strain energy density release rate and current state of damage (Krajcinovic & Lemaitre 1987).

The fatigue damage rate generated by one block of stress cycles has been obtained as follows (Li, Chan & Ko 2000):

$$\frac{\delta D}{\delta N_{bl}} = \sum_{i=1}^{m_{rb}} \frac{[(\Delta\sigma_i + 2\sigma_{mi})\Delta\sigma_i]^{\frac{\beta+3}{2}}}{B(1-D)^\alpha(\beta+3)} \quad \text{For } \sigma_{Mi} = \sigma_m + \frac{1}{2}\Delta\sigma_i \geq \sigma_f \quad (2)$$

where, D is a damage variable and α , B and β are material constants. σ_{Mi} is the maximum stress in the i th cycle, m_{rb} is the number of cycles with the maximum stress over the stress limit to fatigue in the representative block, N_{bl} is the number of blocks and σ_{mi} is the mean stress in the i th cycle.

The increment of fatigue damage generated by a block of stress cycles due to normal traffic is expressed as follows:

$$\Delta D_i = (1 - D_i) - \left\{ (1 - D_i)^{\alpha+1} - \frac{(\alpha+1)}{B(\beta+3)} \sum_{j=1}^{m_{rb}} [(\Delta\sigma_j + 2\sigma_{mj})\Delta\sigma_j]^{\frac{\beta+3}{2}} \right\}^{\frac{1}{\alpha+1}} \quad (3)$$

The increment of fatigue damage generated by a block of stress cycles due to typhoon conditions can be obtained similarly to the fatigue damage increment generated by normal traffic loading as follows:

$$\Delta D_{i+1}^{Ty} = (1 - D_i) - \left\{ (1 - D_i)^{\alpha+1} - \frac{(\alpha+1)}{B(\beta+3)} \sum_{j=1}^{m_{rb}} [(\Delta\tilde{\sigma}_j^{j+1} + 2\tilde{\sigma}_{mj}^{j+1})\Delta\tilde{\sigma}_j^{j+1}]^{\frac{\beta+3}{2}} \right\}^{\frac{1}{\alpha+1}} \quad (4)$$

where, $\tilde{\sigma}_j^{j+1}$ and $\tilde{\sigma}_{mj}^{j+1}$ are stress range and mean stress in the j th cycle of the $i + 1$ th block of stress cycles due to typhoon loading, and m_{rb} is the number of cycles in the considered block. If Miner's Law is applied, the increment of fatigue damage generated by a block of stress cycles due to typhoon conditions can be written as:

$$\Delta D_i^{Ty} = \sum_j^{\tilde{m}_{rb}} \frac{n_j}{N_{Fj}} \quad (5)$$

where, n_j and N_{Fj} are the number of cycles at the stress range $\Delta\tilde{\sigma}_j$ and the relevant number of cycles to failure from the S-N curve for the stress range $\Delta\tilde{\sigma}_j$ respectively, and \tilde{m}_{rb} is the number of cycles with different value of stress range $\Delta\tilde{\sigma}_j$.

The time length of a block designed for the typhoon loading, of course, is no longer a day as defined for normal traffic loading, since the cyclic stress induced by typhoon fluctuates significantly from hour to hour in the amplitude of stress range. It is more appropriate to define the length of a block for the calculation of fatigue damage increment induced by typhoon conditions as an hour according to the above induced strain history analysis.

The calculation of the increment of fatigue damage is carried out for the location of ‘‘SSTLP-09’’ by using Eqs. (4) and (5). Fig. 11 shows normalized results of fatigue damage increment induced by typhoon conditions in which the results are normalized by the constant result of fatigue damage increment due to normal traffic.

It can be observed from Fig. 11 that, firstly, the results calculated from the CDM model are similar to that by Miner’s Law; and secondly, the increment of fatigue damage generated by typhoon conditions at different hours varies significantly. The maximum value is over 3 times of the value for normal traffic loading and occurred at the hourly block between 06:00–07:00. It should be noted that, although the increment of fatigue damage calculated by the CDM model and Miner’s Law has similar results, the values of accumulative fatigue damage would be different for these two models. Miner’s Law is a linear accumulative fatigue damage model and is history independent whilst the CDM model has been verified as a nonlinear accumulative model of fatigue damage under normal traffic loading (Li *et al.* 2001, Chan *et al.* 2001). The accumulation of fatigue damage is history dependent, i.e. the accumulative value of fatigue damage depends not only on the rate of fatigue damage under the present loading but also the present value (or initial value) of fatigue damage. In the view of physical mechanism of fatigue damage, fatigue accumulation is due to fatigue crack initiation and growth. The accumulative rate of fatigue damage depends on the service conditions and deteriorating status of the structure. Therefore, from the view of physical mechanism of fatigue damage, the nonlinear accumulation of fatigue damage is more reasonable, which shows

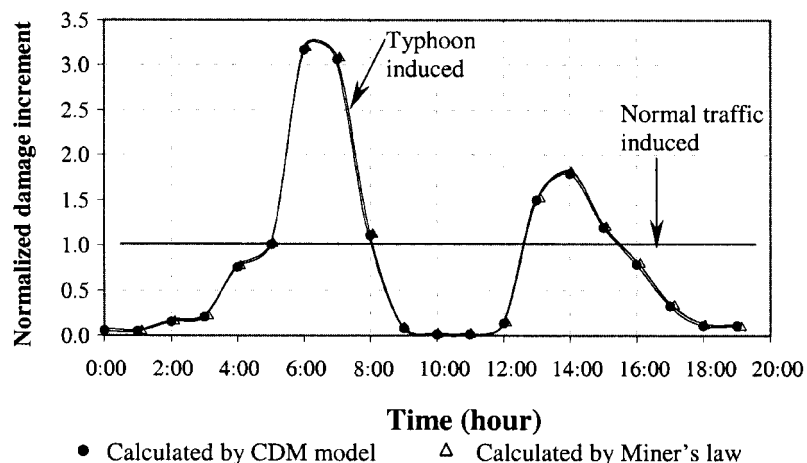


Fig. 11 Normalized fatigue damage increment induced by typhoon and normal traffic

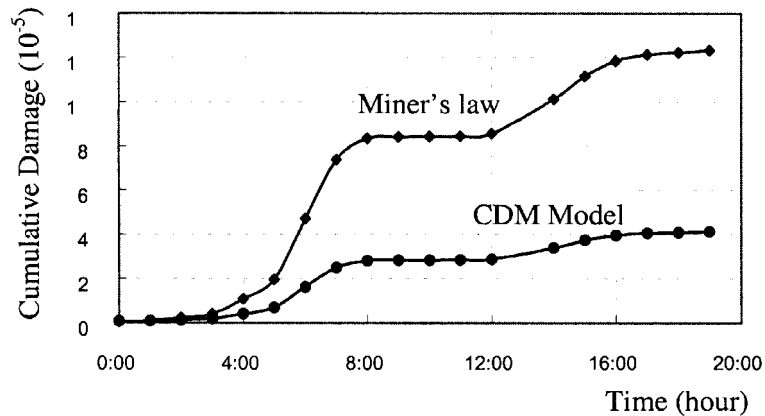


Fig. 12 Curves of cumulative fatigue damage versus time calculated by the CDM model and Miner's law

the accumulative rate of fatigue damage to be small at the beginning of the bridge service then becoming greater during later periods of service. In order to show the accumulation feature of fatigue damage under typhoon loading, the fatigue damage accumulated from the process of the typhoon action is calculated by using Miner's Law and the CDM model respectively. The calculated results are shown in Fig. 11. In the calculation, the present value (or initial value) of fatigue damage before the action of the typhoon is assumed as 0.2. It can be seen that the values of fatigue damage accumulated on the process of the action of the typhoon are different for the results calculated by Miner's Law and the CDM model, and the latter is smaller than the former. The accumulative feature shown in Fig. 12 is similar to the situation for the same bridge deck under normal traffic loading (Li *et al.* 2001 and Chan *et al.* 2001) and at the beginning of the bridge service since the fatigue condition is at the beginning period in the calculation.

7. Conclusions

The present study investigated the effect of a typhoon on fatigue damage of the deck of the Tsing Ma Bridge based on the structural health monitoring system. The measured data of wind and strain response during typhoon Maggie on 7 Jun. 1999 and typhoon York on 16 Sept. 1999, were analyzed to evaluate wind characteristics and typhoon induced fatigue damage of the bridge. Typhoon York is the strongest typhoon since 1983 and the typhoon of longest duration on record in Hong Kong. The hourly strain-time history of the bridge during typhoon York was investigated and compared with that under normal daily traffic loading. The calculation was made in order to obtain the increment of fatigue damage induced by the typhoon. It is found from this work that:

- i. The strain-time history curves during the typhoons have different patterns from that under normal traffic loading. The typhoon induced strain time curves have many cycles of strain range greater than that for normal traffic both in the number of cycles and the amplitudes of strain range. The typhoon induced hourly stress spectrum may generate fatigue cycles approximately equivalent to daily stress spectrum due to normal traffic;

- ii. The influence of a typhoon on the fatigue damage is greater than that for normal traffic, especially for a bridge carrying both highway and railway traffic as the railway remains in-service during a typhoon passing over the bridge. It is, therefore, necessary to evaluate the influence for a long-span bridge located within a typhoon prone region after typhoons attacking.
- iii. For the purpose of accurately evaluating accumulative fatigue damage, a fatigue damage model based on the CDM theory should be applied to assess fatigue using structural health monitoring data. The results of the accumulated fatigue using the CDM model, in the case of typhoon York, are much smaller than that using Miner's Law.

Acknowledgements

Funding support to the project by the National Nature Science Foundation of China (Project Code: 50178019) and the Research Grants Council of the Hong Kong Government (Project Code: PolyU 5042/01E) is gratefully acknowledged. The writers wish to thank the Highways Department of the Hong Kong SAR Government for their support throughout the project.

References

- Aktan, A.E., Grimmelmsan, K.A. and Helmicki, A.J. (1998), "Issues and opportunities in bridge health monitoring", *Proc. of the Second World Conference on Structural Control*, June 28 to July 2, 1998 Kyoto, Japan, ed. Takuji K. *et al.*, **3**, 2359-2368.
- Chan, T.H.T., Li, Z.X. and Ko, J.M. (2001), "Fatigue analysis and life prediction of bridge with structural health monitoring data - Part II: Application", *Int. J. of Fatigue*, **23**(1), 55-64.
- Chan, T.H.T., Ko, J.M. and Li, Z.X. (2000), "Fatigue analysis for bridge-deck sections under blocked cycles of traffic loading", *Nondestructive Evaluation of Highways, Utilities, and Pipelines IV, Proceedings of SPIE*, 7-9 March 2000, **3995**, ed. Aktan, A.E. and Gosselin, S.R., 358-369.
- Dowling, N.E. (1972), "Fatigue failure predictions for complicated stress-strain history", *J. of Materials*, *JMLSA*, **7**(1), 71-87.
- Flint and Neill Partnership (1998), *Lantau Fixed Crossing and Ting Kau Bridge, Wind and Structural Health Monitoring Criticality and Vulnerability Ratings Review*, Highways Department, Government of Hong Kong, Jan. 1998.
- Gu, M., Xu, Y.L., Chen, L.Z. and Xiang, H.F. (1999), "Fatigue life estimation of steel girder of Yangpu cable-stayed Bridge due to buffeting", *J. Wind Engineering and Industrial Aerodynamics*, **80**, 384-400.
- Gurney, T. (1992), *Fatigue of Steel Bridge Decks*, HMSO at Edinburgh Press, London.
- [HREF 1] The Hong Kong Observatory - <http://www.weather.gov.hk/>
- Krajcinovic, D. and Lemaitre, J. (1987), *Continuum Damage Mechanics: Theory and Applications*, Springer, Vienna.
- Lau, C.K. and Wong, K.Y. (1997), "Design, construction and monitoring of the three key cable-supported bridges in Hong Kong", *Structures in the New Millennium*, P.K.K. Lee (ed.), A.A. Balkema, Rotterdam, Netherlands, 105-115.
- Lau, C.K., Wong, K.Y. and Flint, A.R. (2000), "The structural health monitoring system for cable-supported bridges in Tsing Ma control area", *Proc. of Workshop on Research and Monitoring of Long Span Bridges*, April 2000, Hong Kong, 14-23.
- Li, Z.X., Chan, T.H.T. and Ko, J.M. (2000), "Health monitoring and fatigue damage assessment of the bridge deck sections", *Nondestructive Evaluation of Highways, Utilities, and Pipelines IV, Proceedings of SPIE*, 7-9 March 2000, **3995**, ed. Aktan, A.E. and Gosselin, S.R., 346-357.

- Li, Z.X., Chan, T.H.T. and Ko, J.M. (2001), "Fatigue analysis and life prediction of bridge with structural health monitoring data - Part I: Methodology and strategy", *Int. J. of Fatigue*, **23**(1), 45-53.
- Schilling, C.G. *et al.* (1978), "Fatigue of welded steel bridge members under variable-amplitude loadings", *NCHRP Report 188*, National Academy Press, Washington D.C.
- Virlogeux, M. (1992), Wind design and analysis for the Normandy Bridge, in: Larsen, A. (Ed.), *Aerodynamics of Large Bridges*, Balkema, Rotterdam, 183-216.